TECHNICAL NOTE

D-1261

STATIC THRUST AUGMENTATION OF A ROCKET-EJECTOR SYSTEM

WITH A HEATED SUPERSONIC PRIMARY JET

By Albert J. Simonson and James W. Schmeer

Langley Research Center
Langley Station, Hampton, Va.

NATIONAL AERONAUTICS AND SPACE ADMINISTRATION

WASHINGTON   May 1962

NATIONAL AERONAUTICS AND SPACE ADMINISTRATION

TECHNICAL NOTE D-1261

STATIC THRUST AUGMENTATION OF A ROCKET-EJECTOR SYSTEM

WITH A HEATED SUPERSONIC PRIMARY JET

By Albert J. Simonson and James W. Schmeer

SUMMARY

An investigation was conducted in order to evaluate the static
thrust augmentation attainable through the use of a rocket-ejector sys-
tem with a heated supersonic primary jet. This system consisted of a
cylindrical mixing tube in conjunction with a supersonic nozzle having
an expansion ratio of 15 to 1. A hydrogen peroxide gas generator was
used to provide heated nozzle flow. An ejector with a bellmouthed inlet
provided thrust augmentation up to about 18 percent of the primary rocket
thrust, whereas the use of a blunt-lip inlet with elliptical profile pro-
vided augmentation up to 9 percent. Axial withdrawal of the rocket noz-
zle from the ejector provided small gains in thrust augmentation.

INTRODUCTION

Attempts to increase the propulsive efficiency of the rocket engine
have led to various methods of thrust augmentation such as the ejector
and the ducted rocket. (See refs. 1 to 4.) Although the ducted rocket
has potential advantages in specific impulse over the simple rocket at
transonic and supersonic flight speeds, such is not the case at low speeds
because of the lack of ram compression.

One method of circumventing this deficiency might be to provide the
duct with a variable inlet so that at low flight speeds it could operate
as a low-pressure ejector, which does not require combustion within the
duct. The possibilities of augmentation from this method are limited to
low speeds (refs. 1 and 4), but could, nonetheless, be very significant
for some applications. Such a rocket-ejector configuration could, then,
achieve thrust augmentation in two phases: at low flight speeds as an
ejector, whereby free-stream air is accelerated through a converging
inlet by the rocket exhaust; and at higher speeds as a ducted rocket
which requires a divergent inlet and combustion in the duct, since most
rocket exhausts are fuel rich. At very high altitudes, where the con-
figuration is no longer capable of thrust augmentation, the ejector can
be jettisoned. It is, of course, important to realize that any practical

application of such a device requires consideration of the weight penalties involved.

Numerous investigations have shown the entrainment characteristics of subsonic and low supersonic jets; but little experimental evidence pertains to the ability of a highly supersonic jet to entrain air. There are indications that mixing is less rapid when the relative velocity between the jet and the entrained air is high. (See refs. 5 and 6.) The present investigation, therefore, was undertaken to evaluate the augmentation attainable at static conditions with the use of a heated and highly supersonic rocket exhaust. Other work also indicated that axial location of the rocket nozzle with respect to the inlet minimum area of the ejector had an effect on induced airflow; reference 7, for instance, indicates a favorable effect on thrust for some values of withdrawal. In order to indicate the significance of this effect in ejectors capable of handling proportionally larger quantities of air than were used in that investigation, data are presented herein for various degrees of withdrawal.

In the present investigation, a hydrogen peroxide rocket motor provided a heated primary flow (approximately 1,350° F) with an exit Mach number of about 4.0. The primary flow was overexpanded, conforming to the usual condition of high-area-ratio nozzles at sea level. A cylindrical mixing tube was used with two types of ejector inlets.

SYMBOLS

A nozzle cross-sectional area, sq in.

A^* nozzle throat area, sq in.

D mixing-tube diameter, in.

d nozzle withdrawal distance, in. (See fig. 1.)

F_b measured simulated-missile-base thrust, lb

F_E measured ejector thrust, lb

F_R measured rocket-nozzle thrust, including base thrust whenever applicable, lb

F_R' measured rocket-nozzle thrust when unaffected by presence of ejector, lb

$F'_{R,i}$ ideal thrust for complete isentropic expansion of rocket-nozzle flow, $\dfrac{w}{g}\sqrt{2Rg\,\dfrac{\gamma}{\gamma-1}\,t_t\left[1-\left(\dfrac{p_a}{p_c}\right)^{\frac{\gamma-1}{\gamma}}\right]}$, lb

g gravitational acceleration, 32.15 ft/sec^2

l mixing-tube length, in.

p_a standard atmospheric pressure, 14.69 lb/sq in. abs

p_b base static pressure, lb/sq in. abs

p_c nozzle-chamber stagnation pressure, lb/sq in. abs

p_i ejector-inlet wall static pressure, lb/sq in. abs

$p_{t,4}$ local total pressure at station 4 (mixing-tube exit), lb/sq in. abs

p_w nozzle interior wall pressure, lb/sq in. abs

p_4 static pressure at station 4 (mixing-tube exit), lb/sq in. abs

R gas constant for 90.5-percent hydrogen peroxide decomposition products, 69.8 ft-lb/lb-$^{\circ}$R

R_b simulated-base radius, in.

r_b radial distance to any point on simulated base, in.

r_m radial distance to any point in plane of mixing-tube exit, in.

t_a atmospheric temperature, $^{\circ}$F

t_t total temperature of rocket-nozzle flow, $^{\circ}$R

$t_{t,4}$ local total temperature at station 4 (mixing-tube exit), $^{\circ}$F

w measured propellant weight flow, lb/sec

x_1 axial distance downstream of nozzle throat, in.

x_2 axial distance upstream of mixing-tube entrance, in.

y_1 rocket-nozzle-interior ordinate, in. (see fig. 1)

y_2 ejector-inlet-interior ordinate, in. (see fig. 1)

γ arithmetic mean ratio of specific heats for nozzle flow between chamber and nozzle exit, 1.31

θ meridian angle on simulated missile base, deg (see fig. 1)

APPARATUS AND METHODS

Models

The various models were tested at the jet-exit test stand of the Langley 16-foot transonic tunnel. Each configuration consisted of a supersonic nozzle with an expansion ratio of 15 to 1 and an ejector with a cylindrical mixing tube. The mixing tube was fitted with two types of ejector inlets: a bellmouthed inlet, most suitable for static operation, and a blunt-lip inlet with elliptical profile, which is more suitable for operation at forward speeds. The mixing-tube lengths were considerably less than the optimum lengths generally quoted for complete mixing. (For example, see ref. 7.) Figure 1(a) is representative of configurations I to V, in which only the dimensions d and l varied. Figure 1(b) shows configuration VI, which differed from configuration I only in that the external contour of the rocket nozzle was altered and that the simulated missile base was absent. Configuration VII, shown in figure 1(c), consists of the rocket nozzle of configuration VI and an ejector which has the blunt-lip inlet. Photographs showing the essential features of configurations tested appear in figure 2. Changes in alinement between the nozzle and the ejector as a result of heating were measured in preliminary test runs with a cathetometer, and adjustments were made in subsequent runs to compensate for these temperature effects.

Rocket-nozzle flow was generated by a single hydrogen peroxide gas generator. Nozzle-flow total temperature varied between runs from $1,336^\circ$ F to $1,423^\circ$ F. The arithmetic mean ratio of specific heats γ, which is a function of static temperature of the nozzle flow between the

chamber and the nozzle exit, was about 1.31. By using this value for γ, the nozzle-exit Mach number was computed to be about 4.0.

Instrumentation

Thrust forces of the rocket nozzle and the ejector were measured independently by means of a load cell and a balance, respectively. Primary weight flow was measured by means of a vane-type electronic flowmeter located in the hydrogen peroxide supply line. Pressures were measured on the simulated missile base (configurations I to V), on the nozzle interior walls, and on the ejector inlet. The locations of pressure orifices are indicated in figure 1. Not shown in that figure are two orifices in the mixing tube, diametrically opposed and 0.1 inch forward of the exit.

Figure 3 is a sketch of the rakes used to survey the pressures and temperatures of the flow at the mixing-tube exit. The dimensions indicated were obtained by correcting the cold dimensions of the rakes for expansion due to heating by the mixed flow. The tips of the probes were located in the plane of the mixing-tube exit. Test runs, both with and without rakes, established that the presence of the rakes had no measurable effect on the data. Some of the total pressures measured corresponded to supersonic flow, and thus the measurements had to be corrected for the effect of normal shock ahead of the probe. The local ratio of specific heats applicable to this correction was determined according to the local mass-flow ratio and temperature as computed from the temperature-rake measurements. For some of the runs, a static-pressure probe was located toward the center of the mixing tube. (See fig. 3.) The pressure measured by the probe agreed well with the pressures measured by the mixing-tube wall orifices just forward of the exit. On this basis, the wall pressures were taken to represent the static pressure across the exit.

RESULTS AND DISCUSSION

Rocket-Nozzle Performance

Figure 4 indicates the distribution of wall pressures within the rocket nozzle. The nozzle used in all configurations was the same, but the external contour was altered for configurations VI and VII. Thus, the presented pressure distribution is applicable to all configurations where flow separation does not occur. Figure 5 presents the thrust performance of the nozzle with the ejector removed. The differences between

ideal and measured thrust in this case were due largely to overexpansion of the flow. The measured thrust indicated by the figure was used as a standard with which the performance of the seven configurations tested was compared. Small corrections were applied to all measurements of nozzle thrust to compensate for effects of atmospheric-pressure deviation from the standard value of 14.69 lb sq/in. abs.

Rocket-Nozzle—Ejector Performance

Figures 6 and 7 present the combined thrust of the rocket nozzle and the ejector, including the force on the simulated base where applicable. As shown in figure 6, the overall thrust ratio decreased with increasing chamber pressure. Comparisons of configurations I to IV show that the effects of nozzle withdrawal from station 3 (see fig. 1(a)) were beneficial for small amounts of withdrawal throughout the range of chamber pressure covered in the investigation. This information is summarized in figure 7. The optimum amount of withdrawal varied slightly with chamber pressure. The maximum thrust augmentation of 18 percent at $\frac{P_c}{P_a} = 25$ was obtained with the nozzle withdrawn. (See fig. 6.) In accordance with reference 7, the differences in thrust performance due to withdrawal are largely attributed to the change in obstruction of the induced flow at station 3. In the case of configuration I, the obstruction is formed by the nozzle exterior, whereas, for configurations II to V, it is formed by the jet boundary. As the nozzle is further withdrawn, changes in obstruction result from variations in the jet boundary at station 3. The effects of withdrawal were much less pronounced in this test than were demonstrated in reference 7; however, the secondary flow area at station 3 was proportionally larger in the present test. Thus, changes in degree of obstruction had, proportionally, a lesser effect.

Ejector thrust is plotted in figure 8, and the thrust on the simulated missile base is presented in figure 9. Ejector thrust is shown in figure 8 to have decreased consistently as the nozzle was withdrawn, although total thrust increased in some cases, as was shown in figure 7. The explanation for this is that the base-thrust ratios increased as the nozzle was withdrawn. (See fig. 9.) These base-thrust ratios were obtained from integration of base pressures over the base area. Some typical base-pressure distributions are shown in figure 10.

Configuration VI differs from configuration I only in that the external contour of the nozzle was altered and that the simulated missile base was removed. Comparison of the thrusts obtained from these two configurations (fig. 6) indicates that the presence of the base in close proximity with the ejector resulted in only a small thrust penalty. In the presence of the base (configuration I), ejector thrust was somewhat

higher than that for the no-base configuration VI (see fig. 8) which
tended to offset losses due to low pressures on the base. (See fig. 10.)

The thrust augmentation of configuration VII (blunt-lip inlet) was
less than that of the other configurations, as might be expected when
considering the limited inlet area on which reduced pressures can act.
Nevertheless, the thrust augmentation was about 9 percent at $\frac{p_c}{p_a} = 37$.
(See fig. 6.) Figure 11 shows that very low pressures existed on the
blunt-lip inlet, which served to compensate for the lack of frontal area.
(Note shifted ordinate in figure.) There was no significant variation of
these pressures as chamber-pressure ratio was changed; therefore, only
one typical curve is presented in figure 11 for this configuration.

Configuration V was identical to configuration III except that the
mixing-tube length (from station 3 to station 4) was reduced by approxi-
mately the amount of withdrawal d. The resulting loss in thrust aug-
mentation (see fig. 6) emphasizes the need for ample mixing-tube length.
Configurations V and I have the same overall nozzle-ejector length from
station 1 (primary nozzle exit) to station 4 (ejector exit). However,
in configuration V the nozzle was withdrawn (see fig. 6) and this resulted
in a reduced mixing-tube length (station 3 to station 4). Again a loss
in thrust augmentation occurred. Unpublished results of tests of ejec-
tors similar to that of configuration VII, but with various values of
D and with l/D ratios of 2.6 to 2.7, show that due to the limited
mixing lengths, thrust augmentations of less than 1 percent were obtained.
However, it is believed that ejectors with low l/D ratios may improve
if the mixing area between the primary and secondary flows is increased,
as by the use of multiple or noncircular nozzles. Losses in mixing
efficiency may occur, however, if the symmetrical state of flow is dis-
turbed. (See ref. 8.)

Extent of Mixing

Figure 12 shows the distribution of total pressure and total temp-
erature of the flow at the mixing-tube exit. The static pressures at
the exit were found to be practically equal to atmospheric ambient pres-
sure for all test conditions. Comparisons of ratios of total pressure
to static pressure $p_{t,4}/p_4$ for the various configurations indicate
that the flow at the mixing-tube exit generally was far from uniform, a
consequence of the limited mixing-tube length. The figure also shows
that the flow at the mixing-tube exit was capable of further thrust aug-
mentation by virtue of its high kinetic-energy level. Withdrawal tended
to reduce the gradients in both pressure and temperature profiles. At
no time did the flow appear to be significantly asymmetrical. The

temperature distributions of figure 12 indicate the kind of temperatures to which an ejector might be subjected in actual application. Allowance should, of course, be made for the higher jet temperatures of most rocket engines. In this connection, it can be seen that incompleteness of mixing may be desirable as a means of reducing shroud temperatures.

The results obtained for configuration IV (maximum withdrawal) at the minimum chamber-pressure ratio $\frac{p_c}{p_a} = 24.9$ were distinctly different from all other results. In figures 6, 8, and 9, it was not possible to fair these results into a curve with the others of the same configuration. These results are of interest in that they demonstrate the main difficulty of using a high Mach number flow as a primary jet, that is, the increased mixing-tube length required to achieve complete mixing. Nozzle wall pressure measurements indicated that the primary flow at this chamber-pressure ratio alone was separated at the nozzle exit and that its Mach number was comparatively low. Figure 12(d) shows that the total-pressure and temperature distributions were unusually uniform at this chamber-pressure ratio. This uniformity suggests that the low Mach number of the primary flow permitted entrainment to proceed more rapidly, in agreement with references 5 and 6. This condition, together with a withdrawal distance d in which the nozzle flow could entrain air in the manner of a free jet, apparently resulted in the accomplishment of much mixing between stations 1 and 2, prior to entering the ejector inlet. Consequently, the partially mixed jet then occupied so much cross-sectional area that little flow could accelerate along the inlet surface to produce thrust. The reduced entrainment of the secondary flow within the mixing tube is evidenced by the sharp rise in inlet pressures forward of station 3. (See fig. 11.)

An incidental observation made during the test runs was that the ejector reduced noise very noticeably. However, no sound measurements were taken.

SUMMARY OF RESULTS

An investigation of the static thrust obtainable through the use of a rocket-ejector system with a highly heated supersonic jet and a cylindrical mixing tube has indicated the following results:

1. Ejectors using a bellmouthed inlet, most suitable for static conditions, provided a maximum thrust augmentation of about 18 percent at a chamber-pressure ratio of 25, and ejectors using a blunt inlet with elliptical profile, more suitable for forward speeds, provided up to 9-percent thrust augmentation at a chamber-pressure ratio of about 37. In each case, augmentation generally decreased with increasing chamber pressure.

2. Limited axial withdrawal of the rocket nozzle from the ejector-inlet minimum area provided small gains in thrust augmentation, the optimum degree of withdrawal varying slightly with nozzle-chamber pressure.

3. Operation of the ejector in close proximity to a simulated missile base had no significantly detrimental effect on overall thrust.

Langley Research Center,
    National Aeronautics and Space Administration,
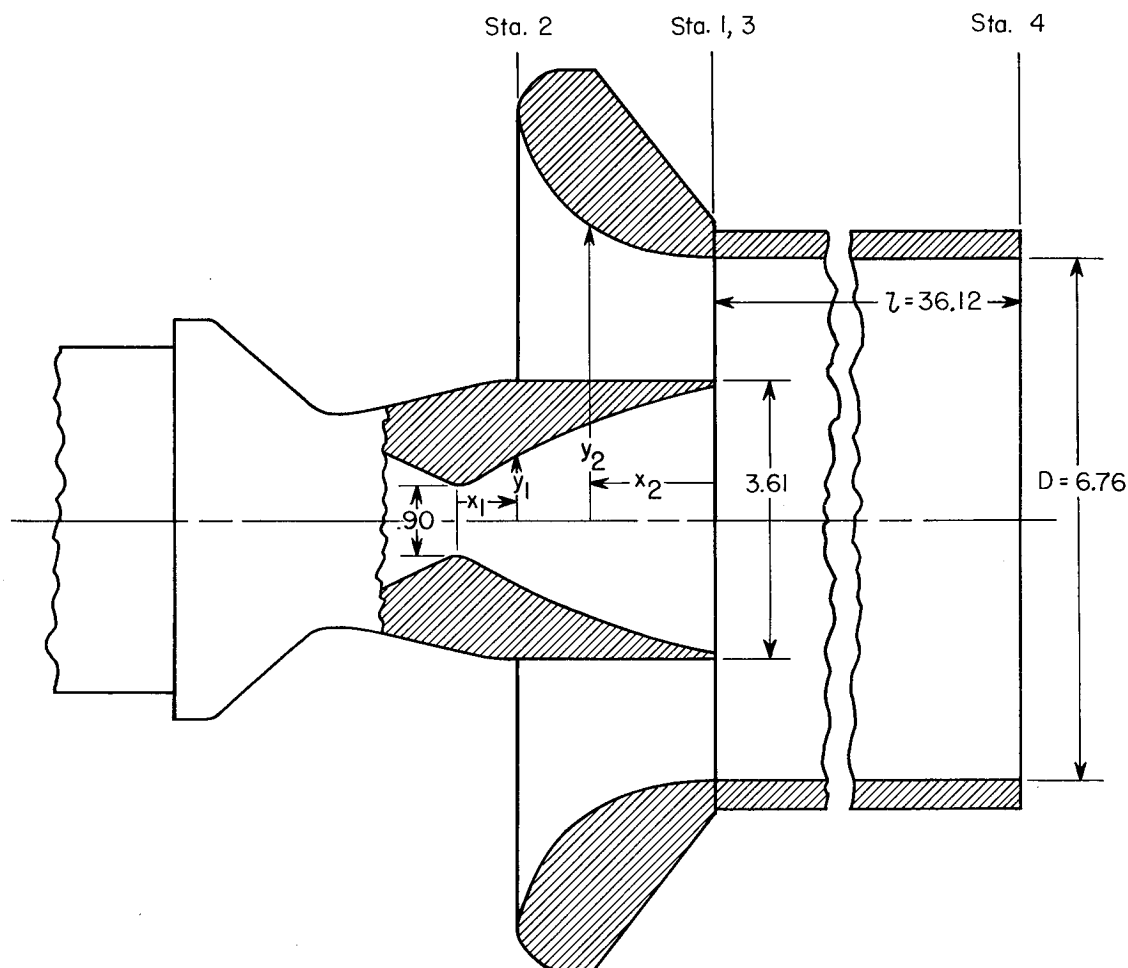   Langley Air Force Base, Va., February 23, 1962.

L
1
8
4
2

REFERENCES

1. Sänger, E.: Air Admixture to Exhaust Jets. NACA TM 1357, 1953.

2. Charyk, Joseph V., and Sutherland, George S.: A Performance Study of the Ram Rocket Power Plant and Related Problems. Tech. Rep. No. 36, Project SQUID, Princeton Univ., Mar. 25, 1952.

3. Kouyoumjian, Walter L., and Tolefson, Donald C.: Preflight and Flight Investigation on a Ducted Solid-Propellant Rocket Configuration at Mach Numbers From 1.56 to 2.14. NASA TM X-29, 1959.

4. Ellerbrock, Herman H., Jr.: General Treatment of Compressible Flow in Ejectors and Example of Its Application to Problem of Effect of Ejector Addition on Thrust of Jet-Propulsion Units. NACA RM L6L23, 1947.

5. Ackeret, J.: Über Luftkräfte bei sehr grossen Geschwindigkeiten insbesondere bei ebenen Strömungen. Helvetica Physica Acta, vol. 1, fasc. 5, 1928, pp. 301-322.

6. Pai, S. I., and Cary, B. B., Jr.: Two Dimensional Jet Mixing of Supersonic Flow. 50 Jahre Grenzschichtforschung, H. Görtler and W. Tollmien, eds., Friedr. Vieweg & Sohn (Braunschweig), 1955, pp. 71-79.

7. Keenan, J. H., Neumann, E. P., and Lustwerk, F.: An Investigation of Ejector Design by Analysis and Experiment. Jour. Appl. Mech., vol. 17, no. 9, Sept. 1950, pp. 299-309.

8. Flügel, Gustav: The Design of Jet Pumps. NACA TM 982, 1941.

Side view of nozzle and ejector

End view of nozzle and base

Pressure-Orifice Locations					
Missile base		Rocket nozzle		Ejector inlet	
θ, deg	r_b	x_1	y_1	x_2	y_2
0	4.75	2.83	1.63	0.25	3.383
0	3.95	2.83	-1.63	.69	3.427
0	3.15			1.16	3.577
0	2.35			1.65	3.866
135	3.55			2.29	4.606
180	2.75				
180	3.55				
180	4.35				

Table of Configurations				
Config.	d	l	d/D	l/D
I	0.00	36.12	0.00	5.34
II	2.43		.36	
III	3.43		.51	
IV	7.50		1.11	
V	3.43	32.62	.51	4.83

(a) Bellmouthed ejector and nozzle with simulated missile base (configurations I to V).

Figure 1.- Sketch of configurations. All linear dimensions are in inches.

L-1842

Side view of nozzle and ejector

Pressure-Orifice Locations			
Rocket nozzle		Ejector inlet	
x_1	y_1	x_2	y_2
0.65	-0.81	0.25	3.383
1.75	1.28	.69	3.427
2.83	1.63	1.16	3.577
2.83	-1.63	1.65	3.866
		2.29	4.606

(b) Bellmouthed ejector and nozzle with simulated missile base (configuration VI). $l/D = 5.34$.

Figure 1.- Continued.
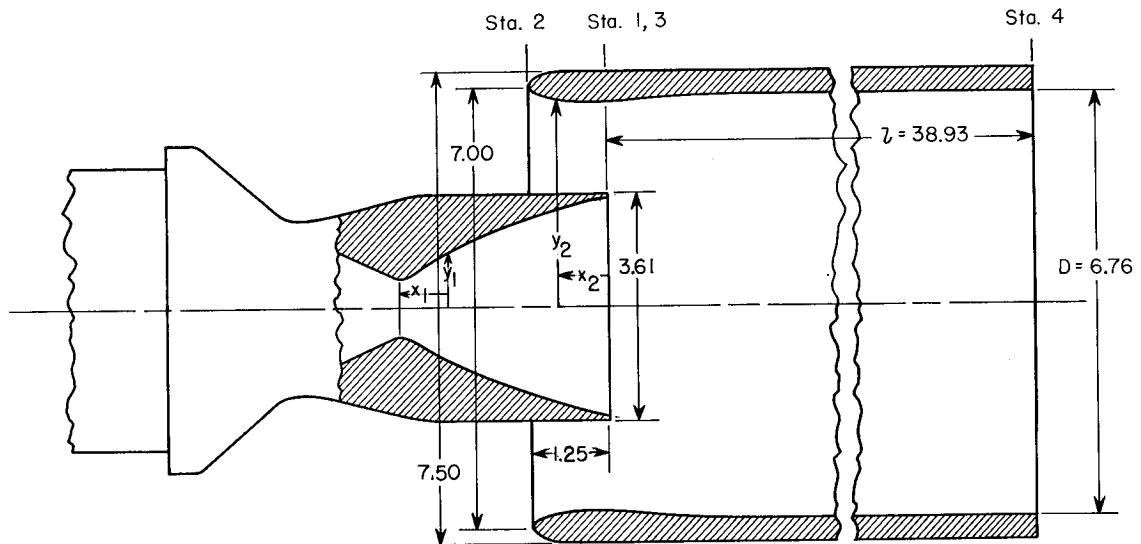
Side view of nozzle and ejector

Pressure-Orifice Locations			
Rocket nozzle		Ejector inlet	
x_1	y_1	x_2	y_2
0.65	−0.81	0.00	3.25
1.75	1.28	.00	−3.25
2.83	1.63	.45	3.26
2.83	−1.63	.45	−3.26
		.88	3.32
		.88	−3.32

(c) Ejector with blunt elliptic inlet and nozzle without simulated
missile base (configuration VII). $l/D = 5.76$.

Figure 1.- Concluded.

L-1842
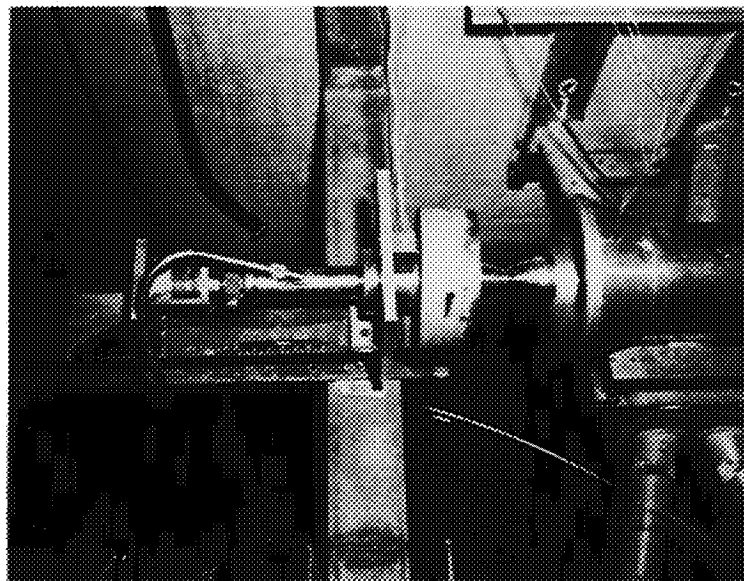
Configuration IV

L-60-4945
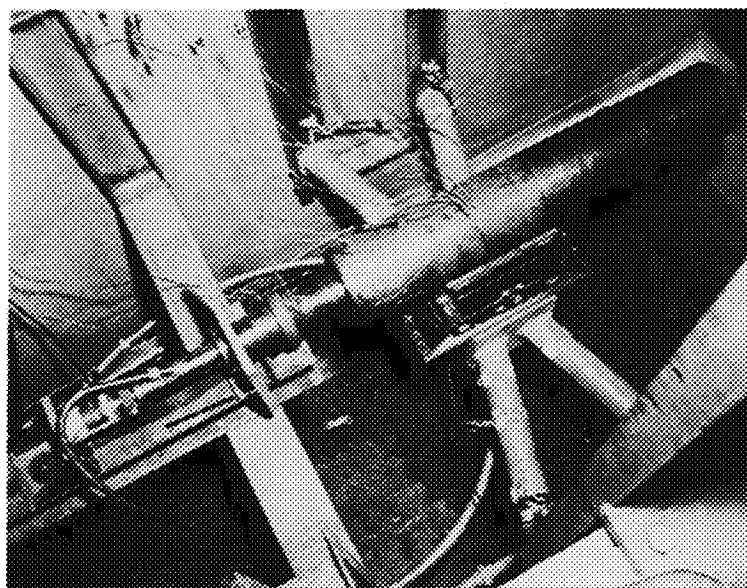
Configuration VII

L-59-7980

Figure 2.- Photographs of two configurations showing gas generator and
rocket nozzle with load cell and ejector with balance.

Front View
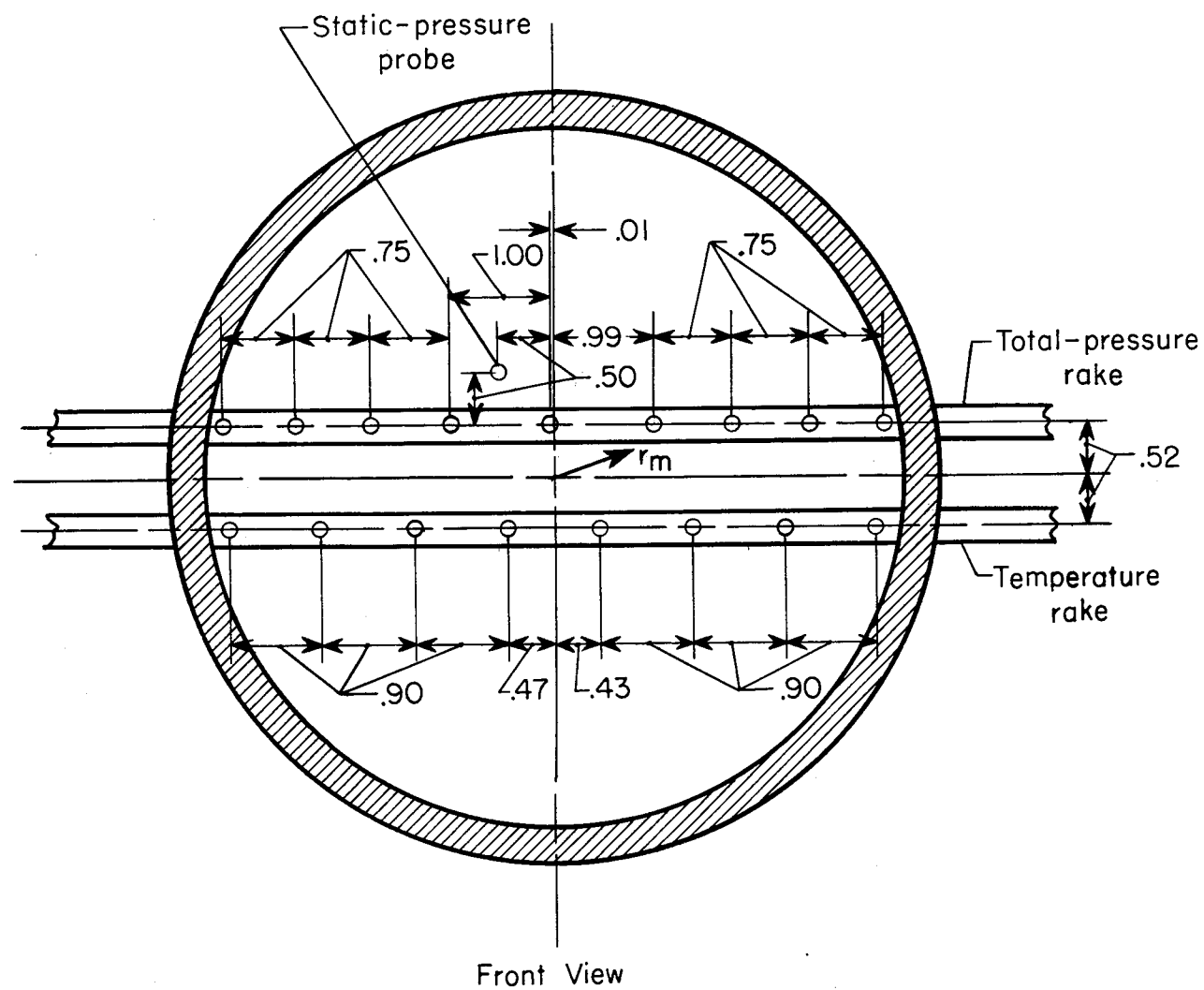
Figure 3.- Sketch of mixing-tube pressure and temperature rakes. All dimensions are in inches.
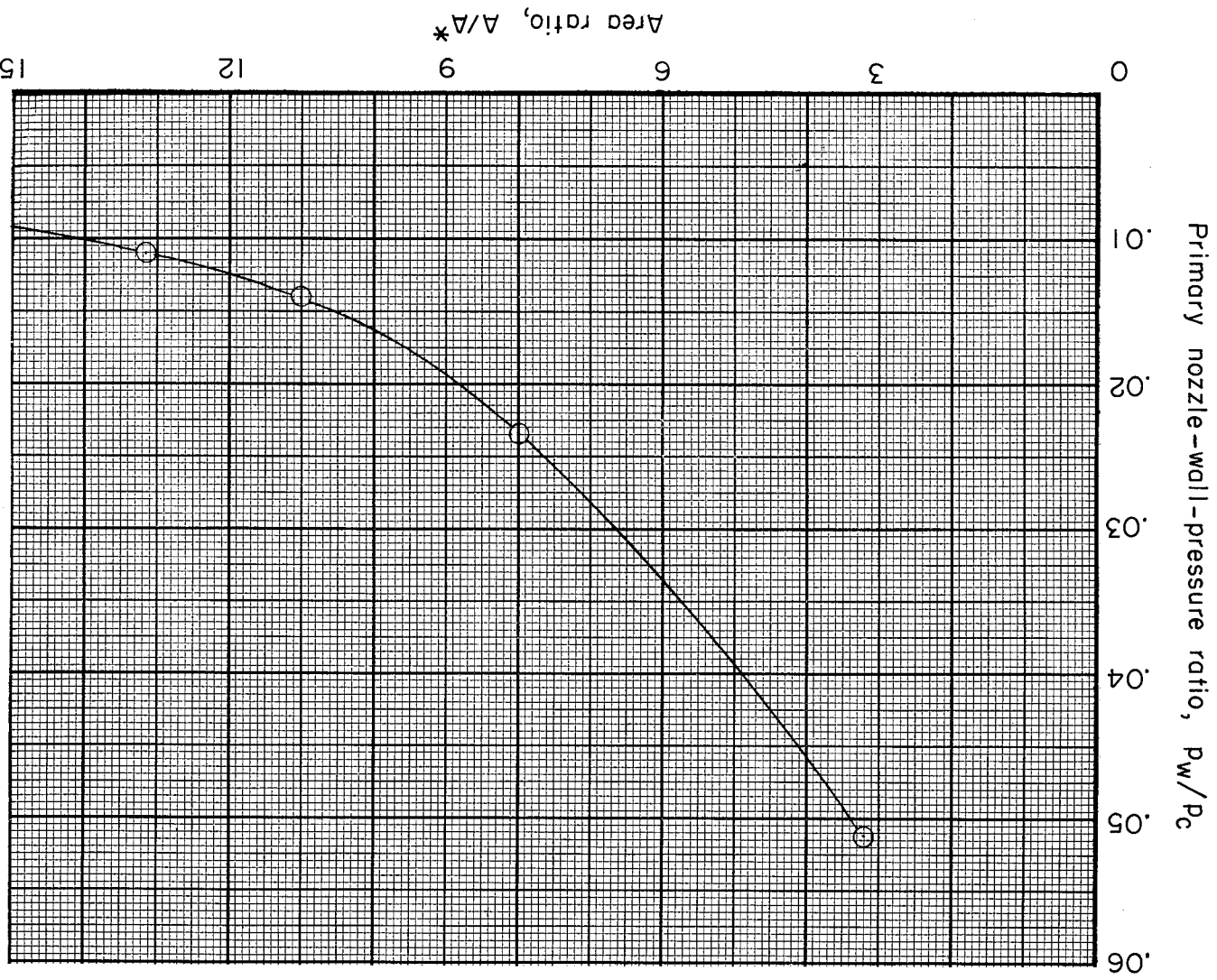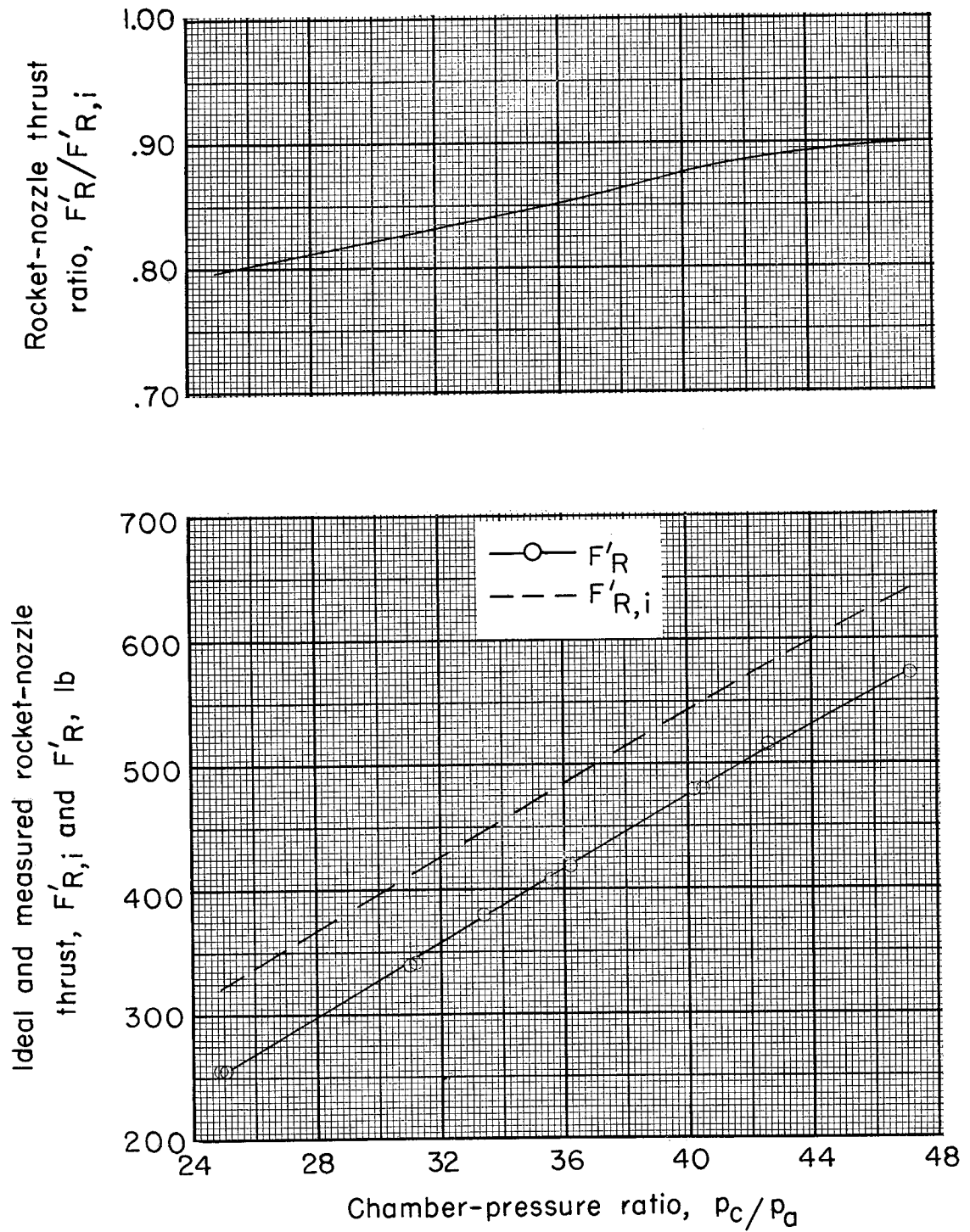
Figure 5.- Thrust performance of rocket nozzle with ejector removed.
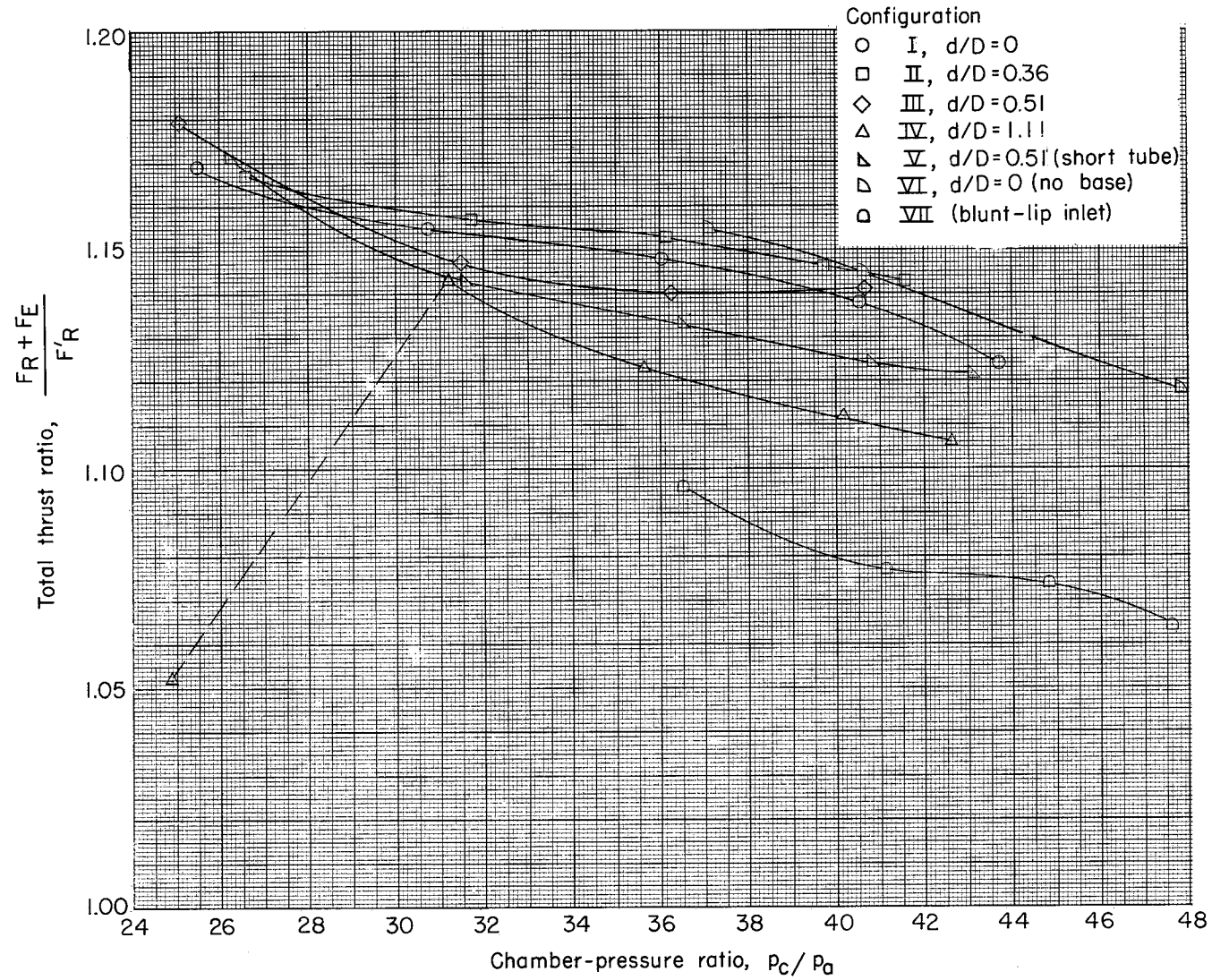
Figure 6.- Variation of thrust of rocket-ejector combination with chamber pressure.
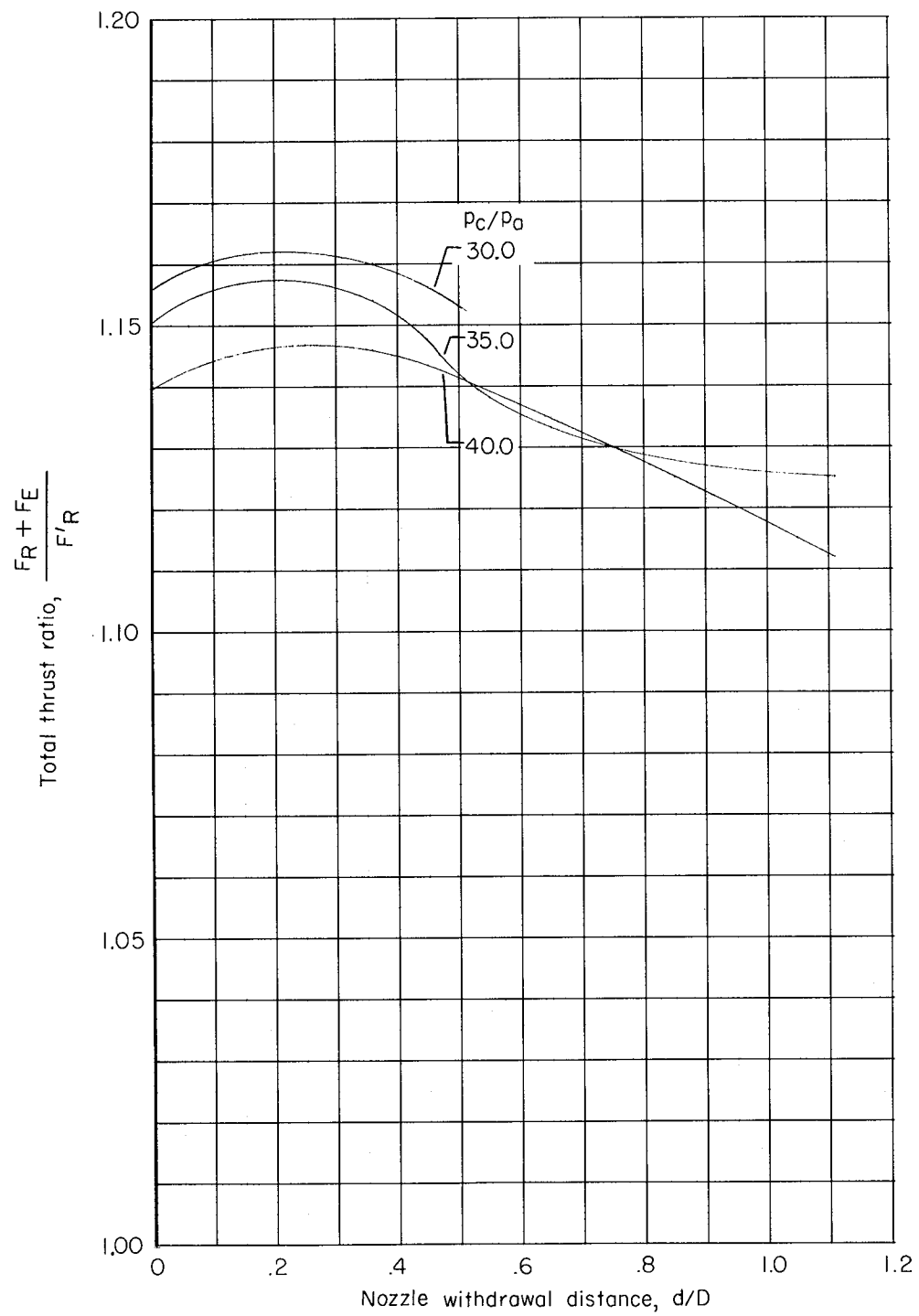
Figure 7.- Variation of thrust of rocket-ejector combination with primary nozzle position.
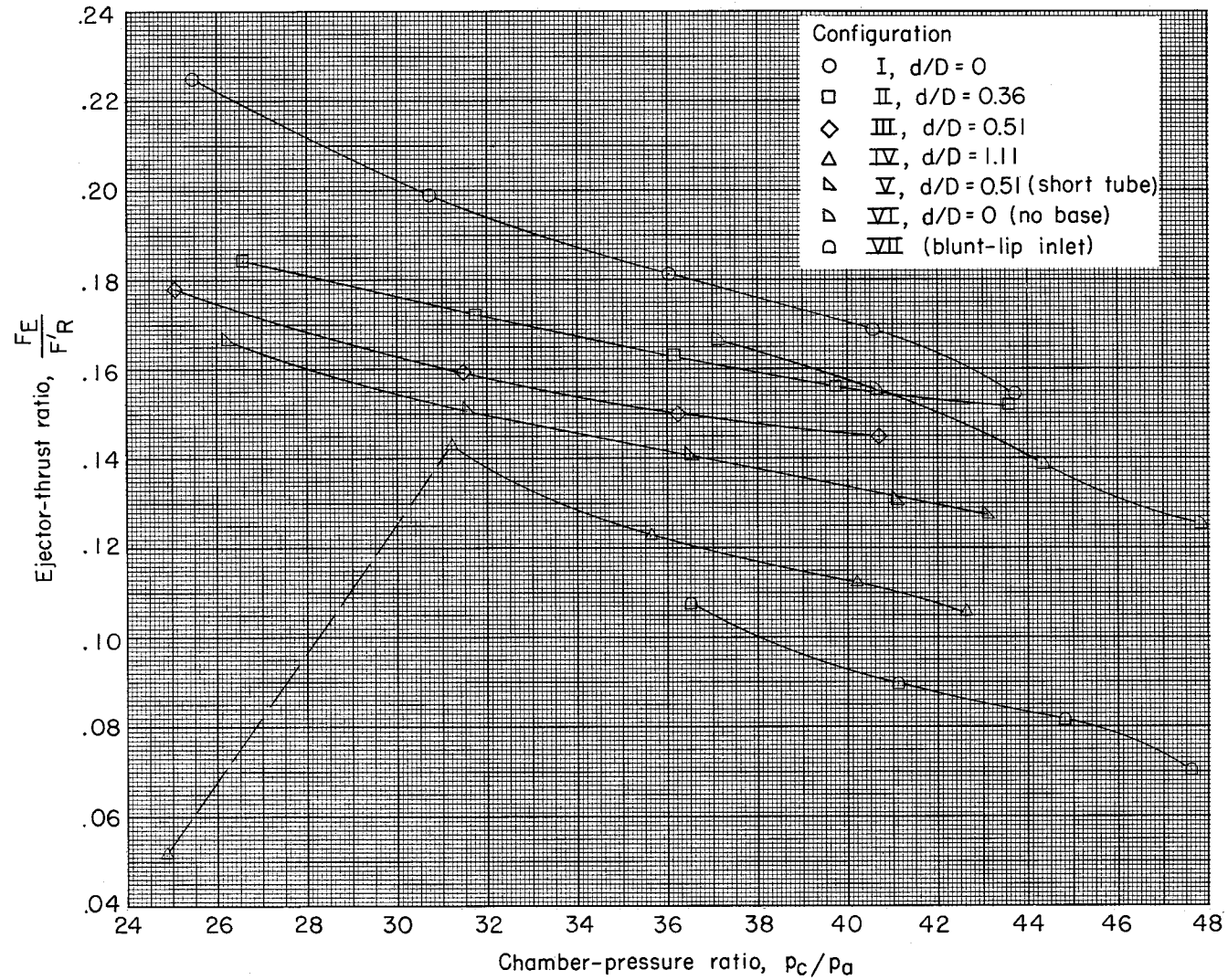
Figure 8.- Variation of ejector thrust with chamber pressure.
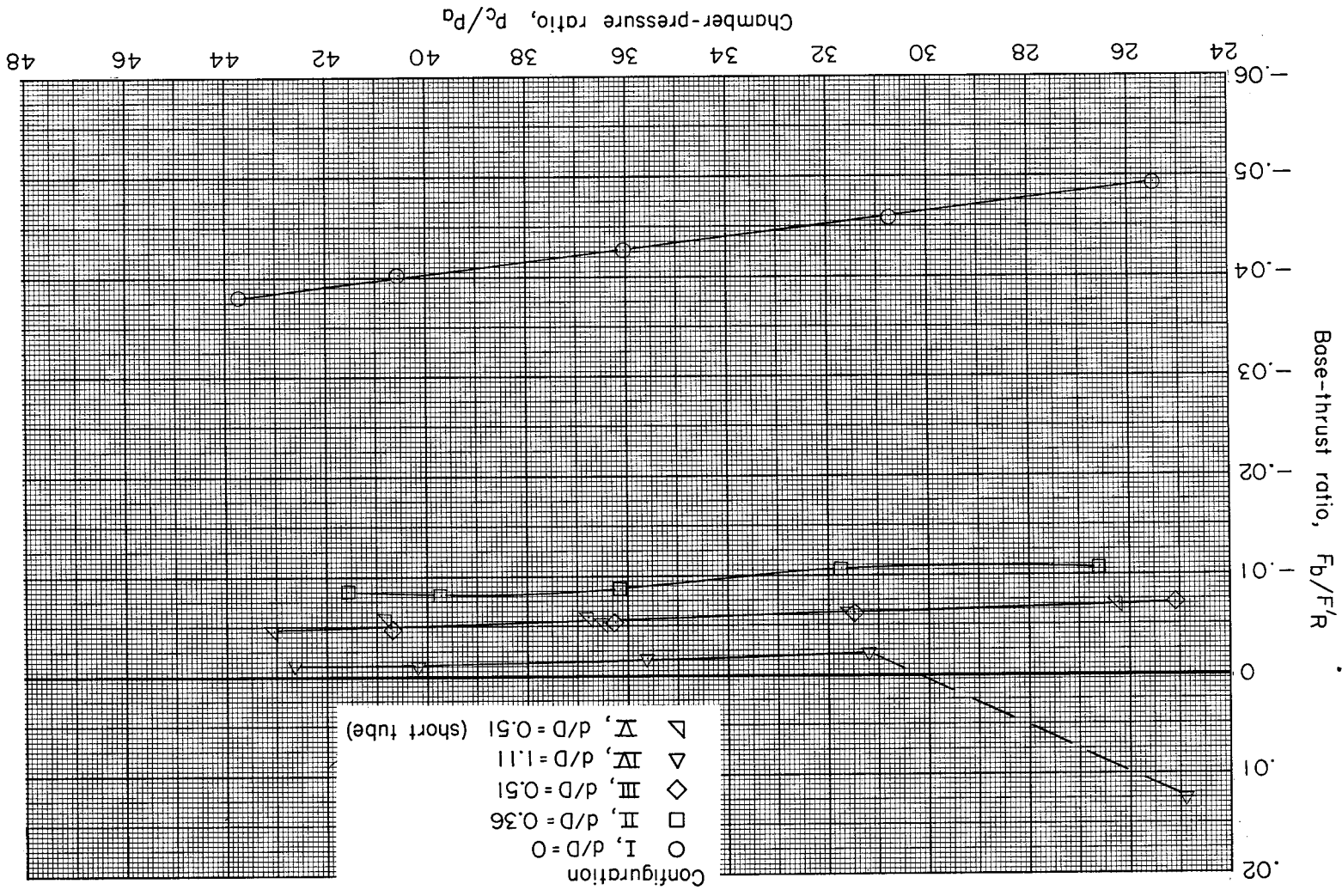
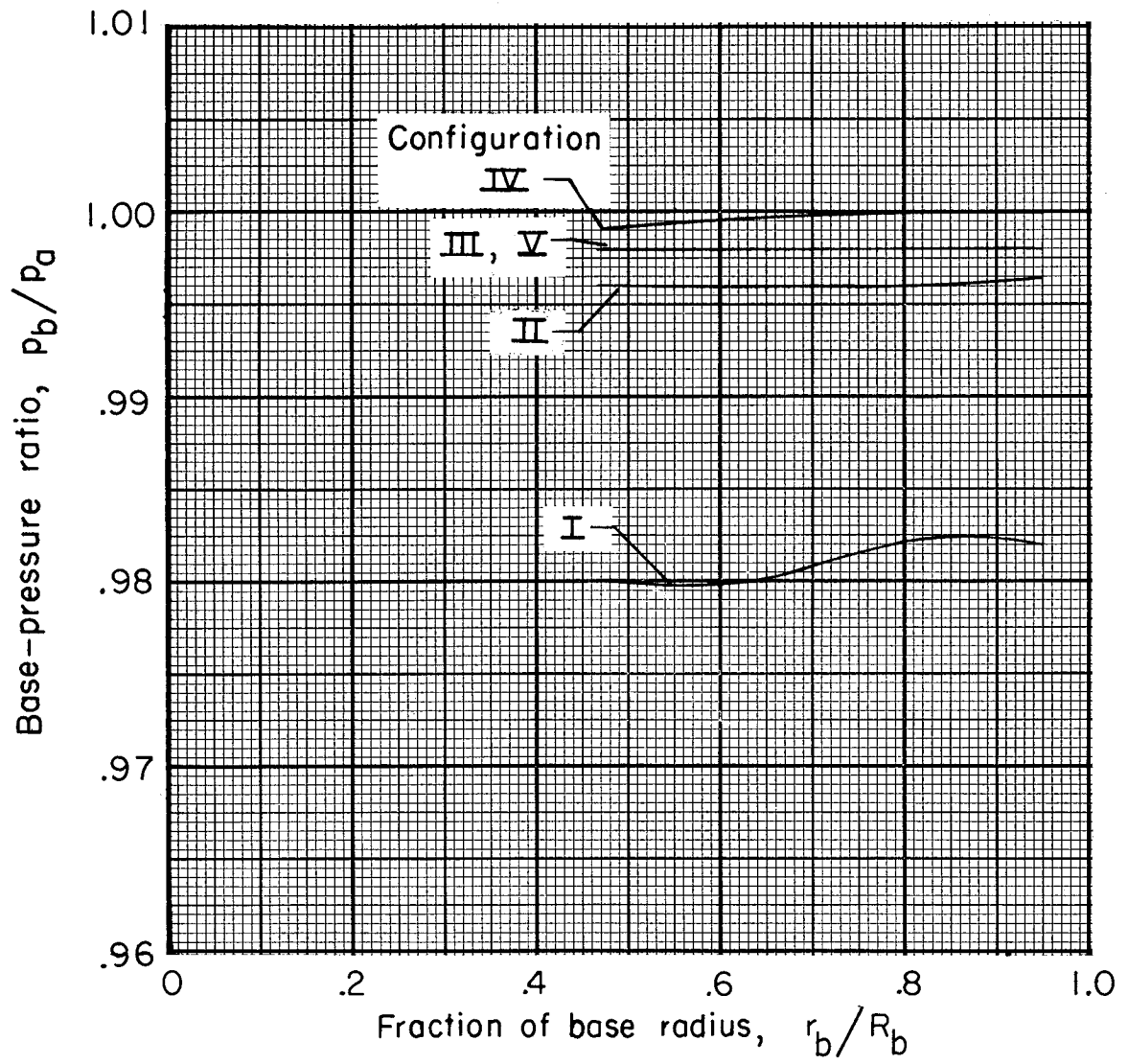Figure 9.- Variation of rocket-base thrust with chamber pressure.

Chamber-pressure ratio, p_c/p_a

Base-thrust ratio, F_b/F'_R

Configuration

O   I, d/D = 0
□   II, d/D = 0.36
◇   III, d/D = 0.51
▽   IV, d/D = 1.11
▽   V, d/D = 0.51   (short tube)
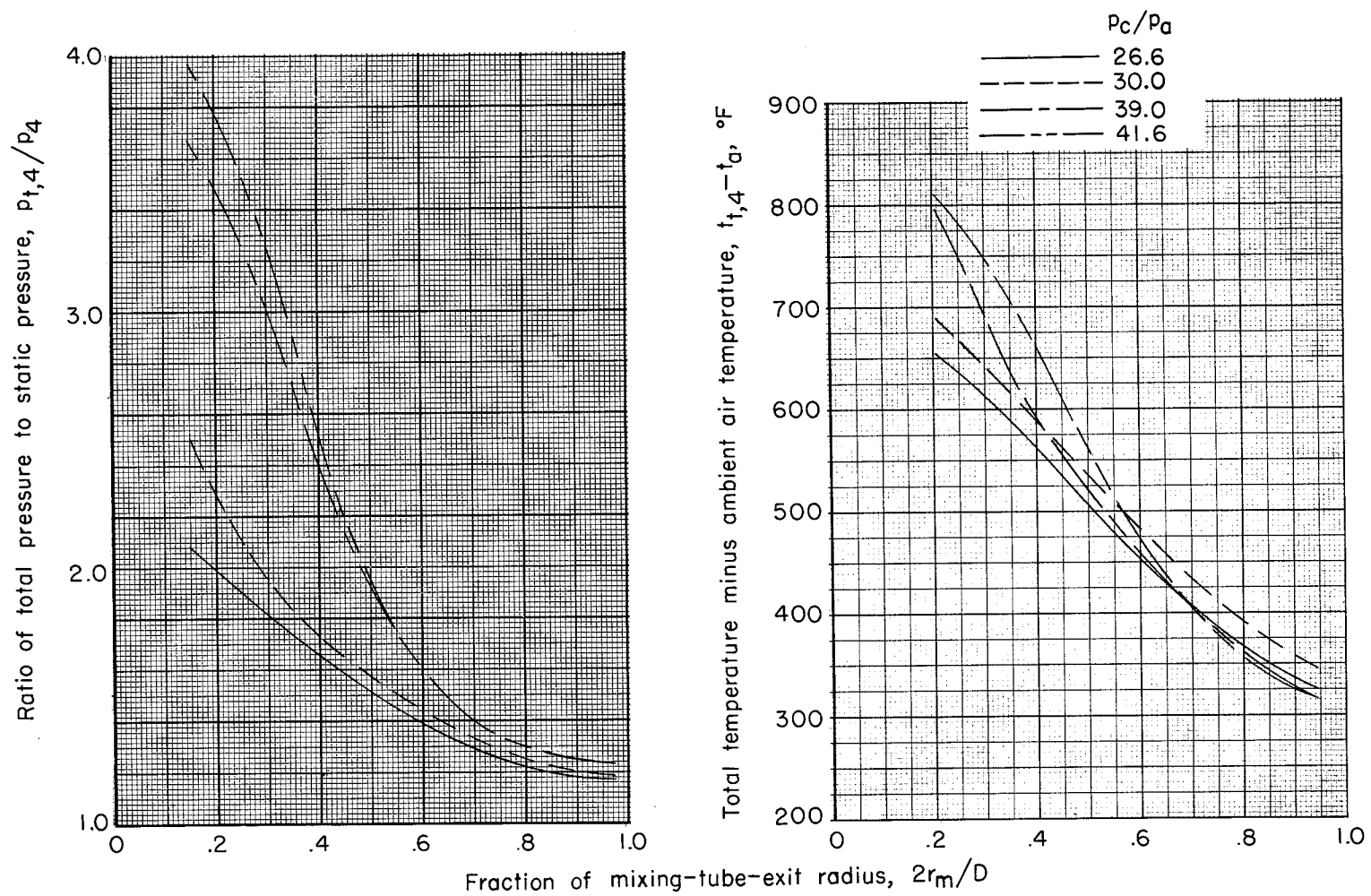
Figure 10.- Typical rocket-base-pressure distribution. $p_c/p_a = 40.8$.
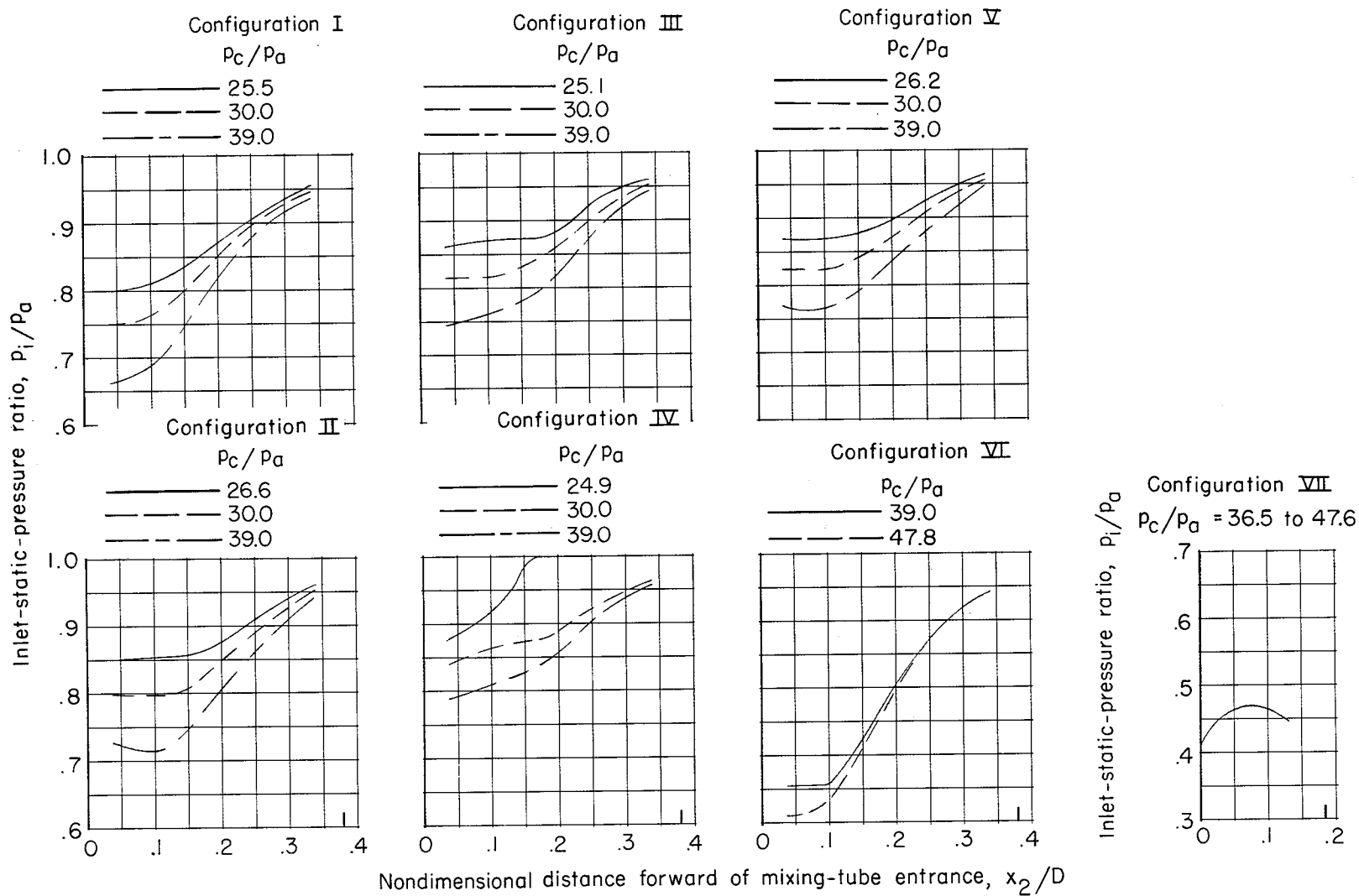
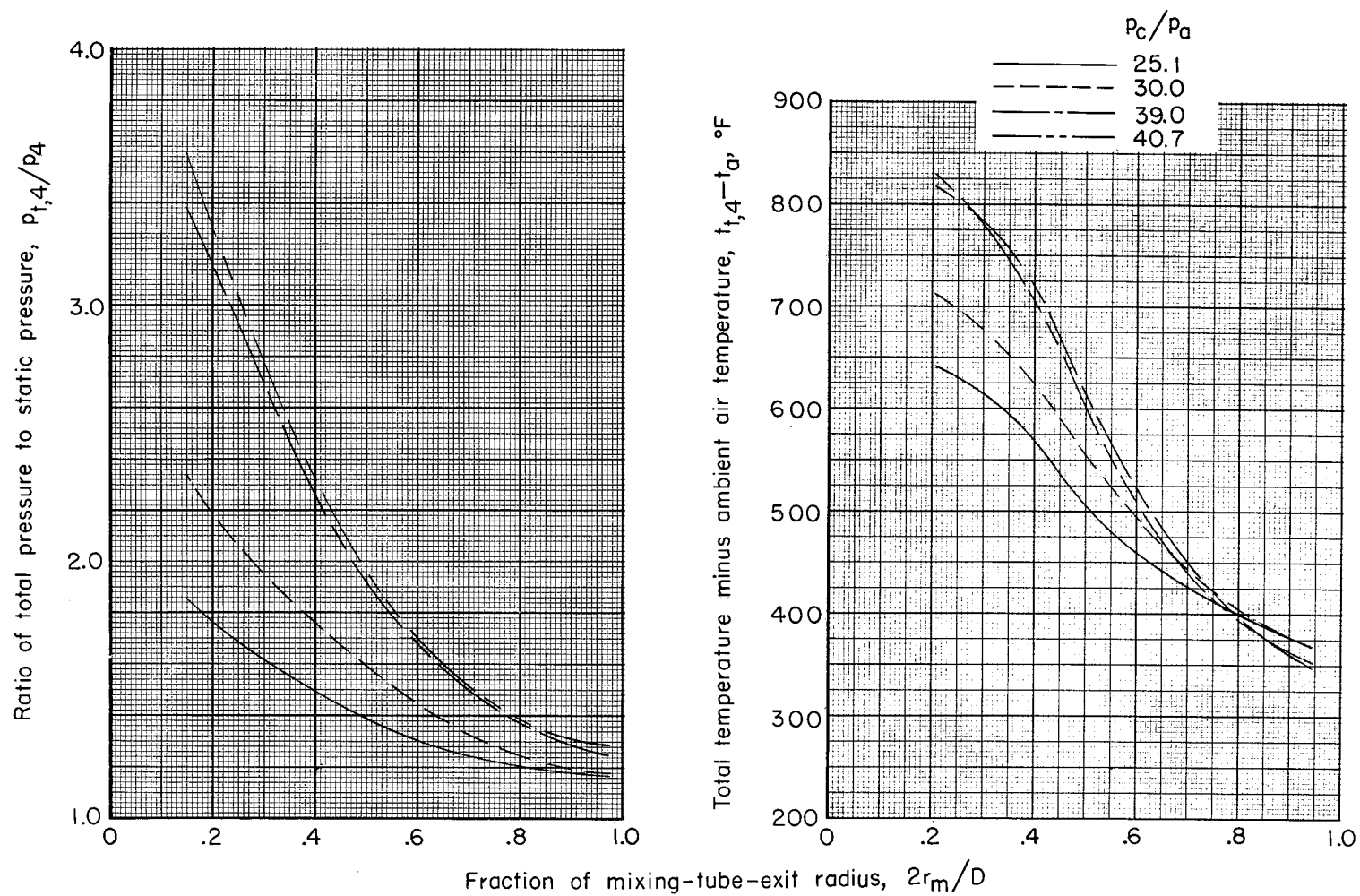Figure 11.- Ejector-inlet pressure distribution. Ticks indicate forward extremity of ejector inlet.
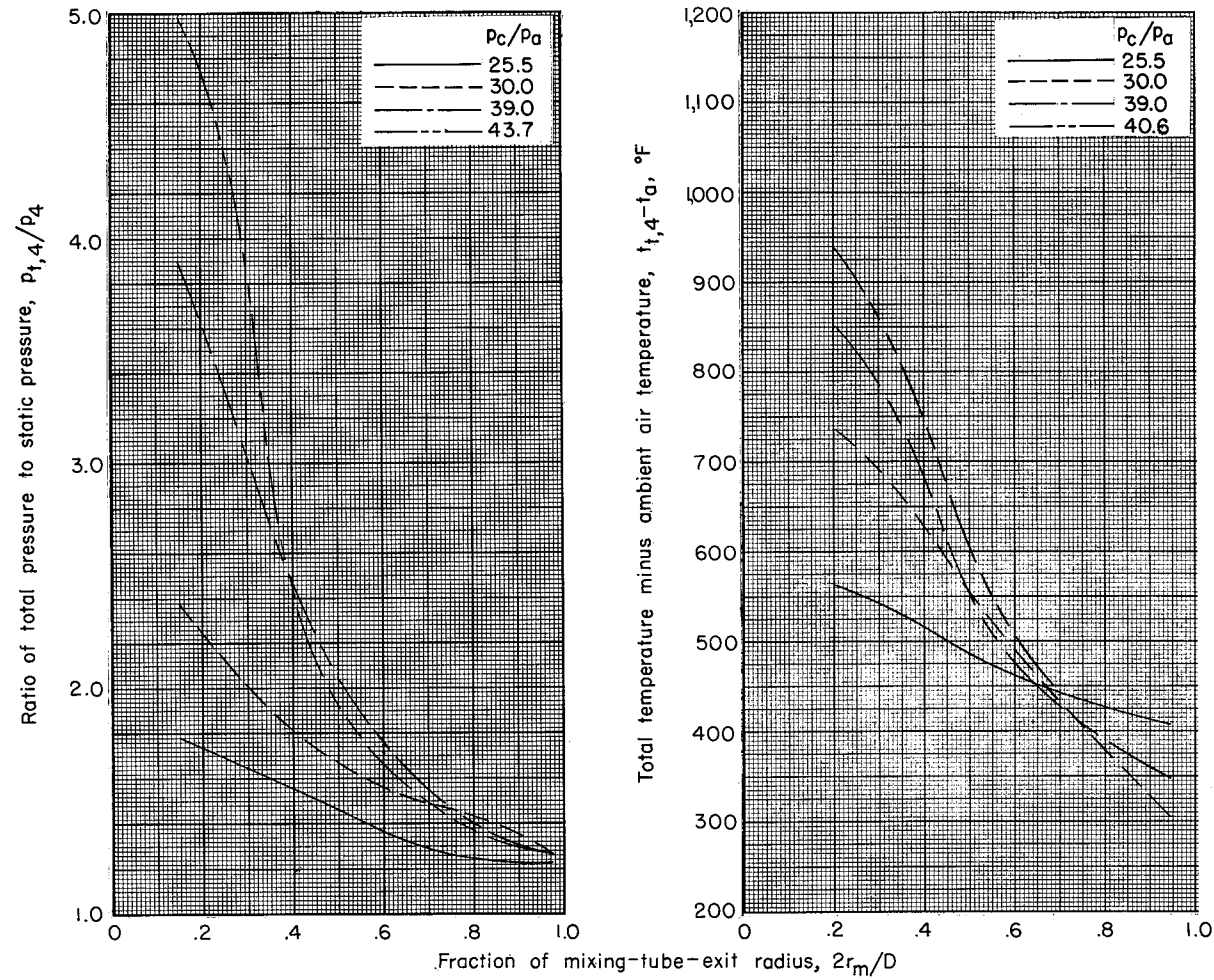
(a) Configuration I.

Figure 12.- Distribution of total pressure and total temperature of flow at mixing-tube exit (station 4).
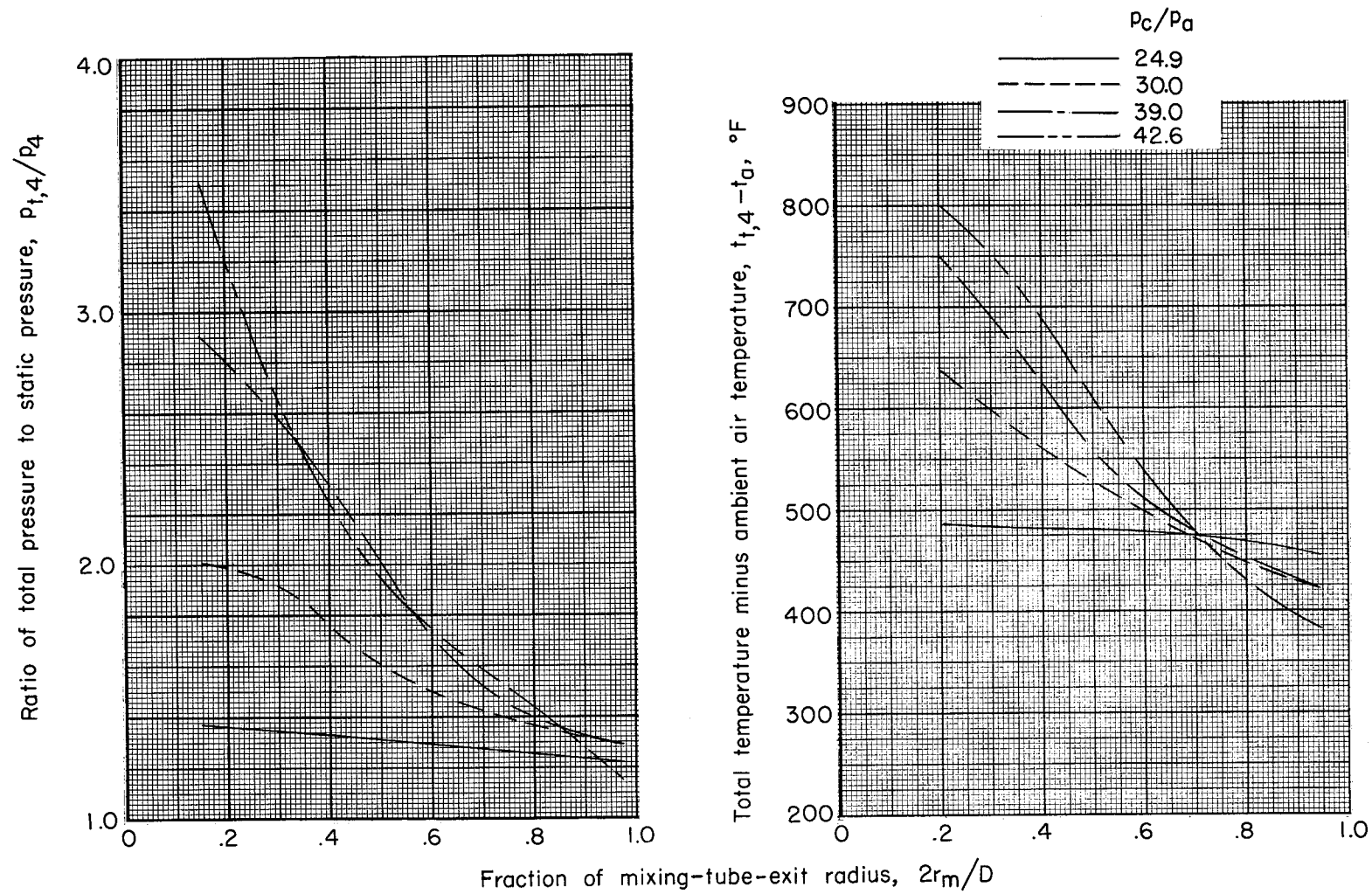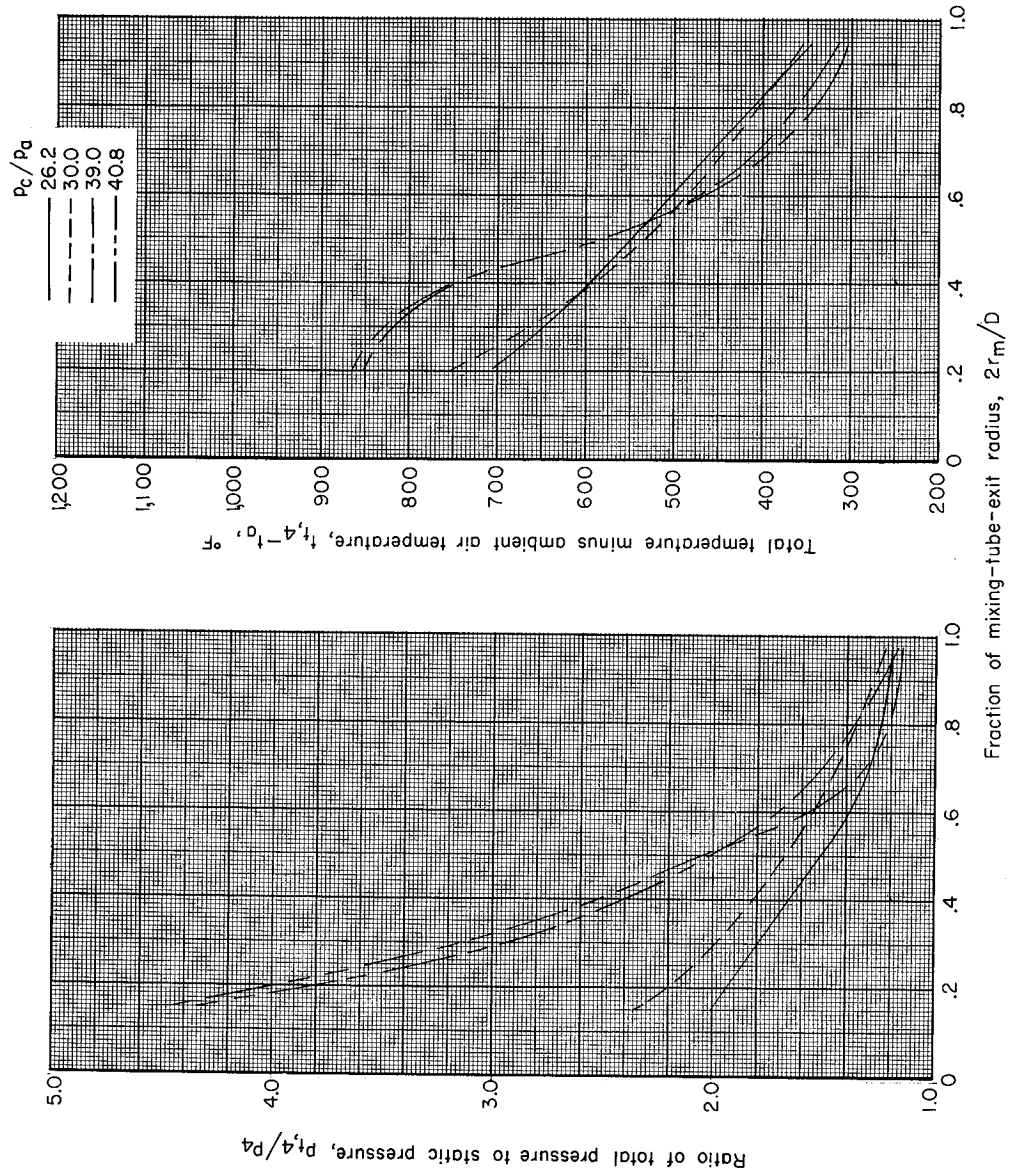
(b) Configuration II.

Figure 12.- Continued.

(c) Configuration III.

Figure 12.- Continued.

(d) Configuration IV.

Figure 12.- Continued.

L-1842

Fraction of mixing-tube-exit radius, $2r_m/D$

Total temperature minus ambient air temperature, $t_{t,4} - t_a$, °F

p_c/p_a

26.2
30.0
39.0
40.8

Ratio of total pressure to static pressure, $p_{t,4}/p_a$

(e) Configuration V.

Figure 12.- Concluded.